UC Davis
UC Davis Previously Published Works

Title

Odorant inhibition in mosquito olfaction mediated by inverse agonists

Permalink

https://escholarship.org/uc/item/4tn6d9hr

Authors

Xu, Pingxi
Choo, Young-Moo
Leal, Walter S

Publication Date

2022-06-01

DOI

10.1016/j.bbrc.2022.04.015

Peer reviewed

Odorant inhibition in mosquito olfaction mediated by inverse agonists

Pingxi Xu,

Young-Moo Choo[1],

Walter S. Leal[*]

Department of Molecular and Cellular Biology, University of California-Davis, Davis, CA 95616, U.S.A.

Abstract

The insect repellent methyl salicylate elicits excitatory responses upon interaction with CquiOR32, an odorant receptor (OR) from the southern house mosquito, *Culex quinquefasciatus.* By contrast, eucalyptol binds to CquiOR32 to generate electrophysiological and behavioral inhibitory responses. In an attempt to identify CquiOR32 variants displaying more robust inhibitory responses for more accurate current-voltage analysis, we sequenced 31 CquiOR32 clones. In the *Xenopus* oocyte recording system, CquiOR32V2/CquiOrco-expressing oocytes yielded eucalyptol-elicited outward (inhibitory) currents relatively larger than methyl salicylate-generated inward (excitatory) currents. Rescuing experiments showed that two of the amino acid substitutions in CquiOR32V2 located in a predicted transmembrane helix of the receptor are determinants of the outward/inward ratios. These findings, along with co-stimulus assays, suggest that odorant and inhibitor may bind to the same binding pocket. Current-voltage relationships obtained with standard perfusion buffer and those devoid of Na^+ or Cl^- indicated that both excitatory and inhibitory currents are mediated, at least in part, by cation. We then concluded that eucalyptol is an inverse agonist, which shifts the open $\Leftrightarrow$ closed equilibrium of the receptor toward the closed conformation, thus reducing the spontaneous activity. By contrast, the binding of methyl salicylate shifts the equilibrium towards the open conformation and, consequently, leads to an increase in cation influx.

Keywords

Culex quinquefasciatus; CquiOR32; binding pocket; methyl salicylate; eucalyptol; I-V curves

[*]Correspondence: Walter S. Leal, wsleal@ucdavis.edu, phone: 530-752-7755.
[1]Present address: R&D Department, Jinju Bioindustry Foundation, Jinju, South Korea

1. Introduction

Chemical signals induce both excitatory and inhibitory responses in olfactory receptor neurons (ORNs) housed in the insect's peripheral olfactory system (antennae, maxillary palps, and proboscis) [1]. Both attractants and inhibitory compounds are crucial for insect behavior. A male moth flying towards a conspecific female's sex pheromone may cease navigation when smelling the chemical signal from another species [2,3]. The vinegar fly is attracted to some food odorants [4] and deterred by others [5]. Mosquitoes find hosts for a blood meal [6] and oviposition sites [7] using attractants (and other signals) but are repelled by other chemicals [8]. These chemical signals of opposite valence are translated into behavioral responses after detection in the peripheral system and processing (integration) in the insect's brain [9–11]. There is growing evidence in the literature that integration of these contradictory chemical signals may also occur at the peripheral olfactory system. That activation of one olfactory receptor neuron (ORN) may cause inhibition of another antennal ORN has been observed in moths [12], beetles [13], the vinegar fly [14], and mosquitoes [15–18], to cite a few examples. At the neuronal level, ephaptic coupling may mediate inhibition in co-located neurons [14,19]. Recently, we reported that odorant receptors (ORs) themselves are activated by some odorants and inhibited by others [15,20]. For example, an odorant receptor from the southern house mosquito, *Culex quinquefasciastus*, CquiOR32, elicited inward currents in the *Xenopus* oocyte recording system when stimulated with the repellent methyl salicylate. By contrast, eucalyptol-elicited positive currents (upward defections in the current traces hereafter referred to as "outward currents"), and eucalyptol-elicited inhibition was manifested in the mosquito behavior. Methyl salicylate-elicited repellency was abolished when the repellent was presented in combination with eucalyptol [15].

Although a fortuitous discovery, the outward currents recorded from CquiOR32 were small and undetectable in an orthologue receptor from the yellow fever mosquito, AaegOR71 [15]. This limitation prevented further examination of its mode of action. Considering that *Cx. quinquefasciatus* has the highest single nucleotide polymorphism of all mosquito species studied thus far [21], we envisioned that there could be CquiOR32 variants displaying more robust inhibitory currents. Out of 31 newly sequenced clones, we identified one variant showing eucalyptol-elicited outward currents larger than methyl salicylate-generated inward currents. Two amino acid substitutions implicated in the relative strength of these currents are located in a predicted transmembrane segment of the receptor, thus indicating that both methyl salicylate and eucalyptol may act on the same binding site. Current-voltage relationships and co-stimulus studies suggested that the binding of methyl salicylate or eucalyptol affects the same cation channels. We hypothesize that while methyl salicylate binding shifts the equilibrium towards the open conformation, thus causing an increase in sodium influx, eucalyptol binding favors the close conformation of the channel, consequently reducing the spontaneous activity.

2. Material and methods

Cloning CquiOR32 variants.

Total RNA was extracted from the antennae of one thousand 4-7 day-old female *Cx. quinquefasciatus* mosquitoes from a laboratory colony [15,22–24] using TRIzol reagent (Invitrogen, Carlsbad, CA). Antennal cDNA was synthesized from 1 μg of antennal total RNA using SMARTer™ RACE cDNA amplification kit according to manufacturer's instructions (Clontech, Mountain View, CA). To obtain full-length coding sequences, PCRs were performed using gene-specific primers. CquiOR32-Fw primer: 5'-ATGTTCACCACTCAAAACAGTCACC-3' and -Rv primer: 5'-TTATATCATAGTCAACGCTTCCTTCAGCA-3'. PCR products were purified by a QIAquick gel extraction kit (Qiagen) and then cloned into pGEM-T vector (Promega). A total of thirty-one plasmids were extracted by a QIAprep spin miniprep kit (Qiagen) and sequenced. To subclone CquiOR32 isoforms into pGEMHE, PCR amplifications were performed using In-Fusion HD Cloning Kit according to the manufacturer's instructions (Clontech). The following PCR primers were designed according to the user manual. CquiOR32-In-Fusion-Fw *Xma*I (underlined) primer: 5'- AGATCAATTC<u>CCCGGG</u>*ACC*ATGTTCACCACTCAAAACAGTC-3' and CquiOR32-In-Fusion-Rv-*Xba*I (underlined) primer: 5'-TCAAGCTTGC<u>TCTAGA</u>TTATATCATAGTCAACGCTTCCTTCA-3'. After transformation, plasmids were extracted using the QIAprep Spin Miniprep kit (Qiagen) and sequenced.

The following PCR primers were used to generate other mutants. CquiOR32-Deletion-Fw: 5'- ATCGTCGAGCTGCACCGAT -3'; CquiOR32-Deletion–Rv: 5'-GTCAACCAGCTCGGATTGC -3'; CquiOR32-L141F restoration-Fw: 5'-GTCCGTTTGTTTTCTGCGC-3'; CquiOR32-#2-L141F restoration-Rv: 5'-CGAAGCAGCAGTAGATCGTG -3'; CqOR32-A148V restoration-Fw: 5'-TCACTTGCGGCAAGTCACT -3'; CquiOR32-A148V restoration-Rv: 5'-CGGAACGCAGAAAACAAACG -3'.

After transformation, plasmids were extracted using the QIAprep Spin Miniprep kit (Qiagen) and sequenced.

Linearized pGEMHE-CquiORs were used as templates to transcribe into capped cRNAs with poly(A) using an mMESSAGE mMACHINE T7 kit from Ambion (Austin, TX).

Two electrode voltage-clamp (TEVC) recordings.

Xenopus oocytes were purchased from EcoCyte Bioscience (Austin, TX). cRNAs were injected into stage V or VI oocytes, which were subsequently incubated at 18°C for 3-7 days in modified Barth' solution [15]. For these recordings, a 10X Ringer's solution was prepared by dissolving NaCl (56.1 g), KCl (1.5 g), $CaCl_2$ (2 g), $MgCl_2•6H_2O$ (10.2 g), and HEPES (2-(4-(2-Hydroxyethyl)piperazin-1-yl)ethanesulfonic acid, 11.9 g) per liter of double distilled water; the final pH was adjusted to 7.6. The perfusion buffer was prepared with a 1 X dilution having [NaCl] 96 mM, [KCl] 2 mM, [$CaCl_2$] 1.8 mM, [$MgCl_2$] 5 mM, and [HEPES] 5 mM. The test oocytes were placed in a

perfusion chamber and challenged with test compounds, including fenchone, eucalyptol, methyl salicylate, cyclohexanone, and the Orco ligand candidate (OLC12), 2-{[4-Ethyl-5-(4-pyridinyl)-4*H*-1,2,4-triazol-3-yl]sulfanyl}-*N*-(4-isopropylphenyl)acetamide [25], also known as VUAA-3 [26]. Compounds diluted into the perfusion buffer were injected (100 μl in 2s) at 1 cm upstream of the flow; the source doses, not the actual doses reaching the oocytes, are reported. Currents were amplified with an OC-725C amplifier (Warner Instruments, Hamden, CT), low-pass filtered at 50 Hz, and digitized at 1 KHz. Data were acquired with Digidata 1440A and pCLAMP 10 software (Molecular Devices, LLC, Sunnyvale, CA). Odorant-induced currents at the holding potential of −80 mV were recorded. To obtain current-voltage relationships, induced currents were recorded with the holding potential at −80, −60, −40, −20, 0, 20, and 40 mV. Sodium-free perfusion buffer was prepared as described above for the standard perfusion buffer by using N-methyl-D-glucamine (Sigma, Milwaukee, WI) at 96 mM instead of sodium chloride. Chloride-free perfusion buffer was prepared with sodium gluconate (Sigma), which replaced all sources of chloride anions to perfusion ringer having a composition of [NaGlu] 96 mM, [KGlu] 2 mM, [CaGlu$_2$] 1.8 mM, [MgGlu$_2$] 5 mM, and [HEPES] 5 mM, pH adjusted to 7.6.

Co-application of odorants.

Perfusion and injection buffers were prepared from the same 10 X Ringer's solution (see above). They had no stimulus (standard perfusion buffer), methyl salicylate alone (injection buffer without continuous eucalyptol stimulus), eucalyptol alone (for perfusion with a continuous stimulus), and methyl salicylate and eucalyptol (for methyl salicylate injection under continuous eucalyptol stimulus). Samples were applied with a Valve Control System (Warner Instruments). After perfusion buffer equilibrated for 1 min and 40 s, compounds were applied four times during 3 min and 20 s. First, CquiOR32/CquiOrco- or CquiOR32V2/CquiOrco-expressing oocytes were challenged with methyl salicylate alone. Then, the standard perfusion buffer was replaced with a perfusion buffer containing the desired concentration of eucalyptol (0.1, 1, 10, or 100 μM). After the baseline stabilized, a methyl salicylate sample was injected. The injected sample had the desired concentration of methyl salicylate (100 μM) and the same dose of eucalyptol as the perfusion buffer (0.1, 1, 10, or 100 μM). The responses to metyl salicylate alone (under standard perfusion buffer) were recorded before and after co-exposure to eucalyptol. A complete set of data (five replicates) was obtained with each oocyte. To minimize a possible buffer effect, data obtained with different batches of buffers were first normalized before they were combined. Specifically, the mean response to methyl salicylate control (no eucalyptol) was used to normalize the responses to control and the tested dose of eucalyptol. Thus, responses to eucalyptol are displayed as relative responses elicited by methyl salicylate.

Statistical analysis and graphical preparations.

Prism 9.3.1 from GraphPad Software (La Joya, CA) was used for statistical analysis and graphical preparations. All data are presented as mean ± SEM. A dataset that passed the Shapiro-Wilk normality test was analyzed by t-test; otherwise, data were analyzed by Wilcoxon matched-pairs signed-rank. To obtain reverse potentials, I-V data were analyzed by simple linear regression. Standard errors were calculated by dividing the 95% confidence

intervals by 3.92. For displays of the experimental data, curve fitting was done with centered third-order polynomial (cubic).

3. Results and discussion

Prospecting for CquiOR32 variants.

In our attempt to identify variants displaying strong outward currents (showing deflection upward in the current trace), we sequenced 31 CquiOR32 clones, of which 12 were identical to the previously reported wild-type CquiOR32 (KM229539) [15]. Their amino acid sequences showed 99.75% identity to CquiOR32 in VectorBase. Specifically, out of the 397 amino acid residues, the VectorBase predicted protein sequence differs in one amino acid residue (Ile-249 in CPIJ004156 and Val-249 in KM229539). Nine clones had nonsense mutations and, therefore, were considered pseudogenes. Six clones (variants) had one single amino acid difference: CquiOR32M288T (GenBank, MG593060; initially identified as variant #8), CquiOR32H161L (MG593061, variant #10), CquiOR32Y350C (MG593062, variant #12), CquiOR32S127P (MG593064, variant #20), CquiOR32W284R (MG593065, variant #25), and CquiOR32L299P (MG593066, variant #26). Three variants differed in two amino acid residues: CquiOR32D62A;R233L (MG593063, variant #14), CquiOR32E13V;L305P (OM370996; variant #15), and CquiOR32D62A;D119V (MG593067, variant #30). One variant differed in two amino acid residues and showed an insert: CquiOR32D250_I251insIVELVD;F141L;V148A (MG593059, variant #2).

Next, we co-expressed each variant with the obligatory coreceptor Orco, CquiOrco, and challenged the oocytes with methyl salicylate, eucalyptol, other agonists, and inhibitors, and the Orco ligand candidate OLC12 [25], also known as VUAA-3 [26].

CquiOR32D62A;R233L/CquiOrco-, CquiOR32E13V;L305P/CquiOrco-expressing oocytes did not elicit currents when challenged with agonists, inhibitors, or OLC12. Oocytes co-expressing CquiOR32M288T or CquiOR32W284R with CquiOrco gave very weak responses to methyl salicylate and no response to eucalyptol. CquiOR32S127P/CquiOrco-expressing oocytes elicited week responses when challenged with methyl salicylate or eucalyptol. CquiOR32H161L/CquiOrco-expressing oocytes gave moderate responses to methyl salicylate but no response to eucalyptol. The response profiles obtained with CquiOR32L299P/CquiOrco- or CquiOR32D62A;D119V/CquiOrco-expressing oocytes were similar to that recorded with the wild type receptor, i.e., relatively large responses to methyl salicylate than eucalyptol. Interestingly, CquiOR32Y350C/CquiOrco-expressing oocytes gave no response to eucalyptol, but elicited larger currents than the wild-type receptor when stimulated with methyl salicylate and other agonists. More importantly, CquiOR32D250_I251insIVELVD;F141L;V148A (hereafter referred to as CquiOR32V2) was relatively more sensitive to eucalyptol than methyl salicylate. As shown in Fig. 1, CquiOR32V2/CquiOrco-expressing oocytes gave robust outward currents when challenged with fenchone or eucalyptol and moderate inward currents when stimulated with methyl salicylate.

Insights on structural determinants of dual currents.

The insert in CquiOR32V2 appears in the predicted intracellular loop-2, and residues Leu-141 and Ala-148 are substitutions in the predicted [27] transmembrane domain-3 (TM-3) (Figs. 1). To identify possible structural determinants of the outward/inward current profiles, we deleted the insert and compared the responses of the truncated (CquiOR32V2del I151_D156 = CquiOR32F141L;V148A) (Fig. 2B) and intact Variant2 (CquiOR32V2) (Fig. 2A) using the *Xenopus* oocyte recording system. The ratio of the eucalyptol/methyl salicylate-elicited currents did not change significantly. These data suggest that the substitutions in TM-3, rather than the insert, play a role in the high eucalyptol-to-methyl salicylate responses. Specifically, the recorded ratios of the outward current elicited by eucalyptol to the methyl salicylate-generated inward currents at 1 mM were 1.66±0.16 with CquiOR32V2 (Fig. 2A, N=4) and 1.22±0.08 (Fig. 2B, N=5) with the mutant with the insert deleted (P=0.0635, unpaired, two-tailed, unpaired, Mann-Whitney test). Next we compared the responses to CquiOR32V2 with V2 one-point mutants, i.e., CquiOR32D250_I251insIVELVD;F141L;V148A (V2), CquiOR32D250_I251insIVELVD;F141L (residue at 148 rescued to wild-type), and CquiOR32D250_I251insIVELVD;V148A (residue at 141 rescued to wild-type). While CquiOR32V2 showed a profile with a relatively larger response to eucalyptol than methyl salicylate at the tested doses of 1 μM to 1 mM (Fig. 2A), CquiOR32D250_I251insIVELVD;F141L/CquiOrco-expressing oocytes (Fig. 2C) showed a response profile similar to that of CquiOR32 wild-type. Specifically, mutating the residue 148 in CquiOR32V2 to Val (as in the wild type receptor) restored the original profile with relatively larger inward currents elicited by methyl salicylate and smaller outward currents generated by eucalyptol. The measured eucalyptol-to-methyl salicylate ratio at 1 mM (0.37±0.04 (N=4) significantly differed from the ratio obtained with CquiOR32V2 (Fig. 1A) (P=0.0011, two-tailed, unpaired, Mann-Whitney test). On the other hand, the profile obtained with oocytes co-expressing CquiOR32D250_I251insIVELVD;V148A and CquiOrco (Fig. 2D) showed an intermediate eucalyptol-to-methyl salicylate ratio of 0.86±0.05 (N=4), which is also significantly different from the ratio measured with CquiOR32V2 (P=0.0159, two-tailed, unpaired, Mann-Whitney test). In short, a mutant of CquiOR32V2 having the residue 141 mutated to Phe (as in the wild-type receptor) did not completely restore the original profile of CquiOR32 wild-type but differed from the profile measured with CquiOR32V2. We then surmised that both residues, particularly Ala-148, are important to elicit a strong outward current. To further test this hypothesis, we prepared two other mutants, CquiOR32V148A and CquiOR32F141L, which differ from the wild-type receptor (CquiOR32, KM229539) in a single amino acid residue each. CquiOR32F141L/CquiOrco-expressing oocytes gave a profile with a relatively larger response to methyl salicylate than eucalyptol (eucalyptol-to-methyl salicylate ratio at 1 mM, 0.36±0.07) (Figs. 2A). On the other hand, the eucalyptol-to-methyl salicylate ratio in CquiOR32V148A was 1.00±0.33 at 1 mM. These data suggest that Ala-148 and, to some extent, Leu-141 contribute to the enhanced outward currents.

We have previously conjectured that inhibitory compounds could be negative allosteric modulators. Given the dissimilarity of the chemical structures, we assumed that agonists and inhibitors would bind to different binding sites. The current findings showing that the

predicted TM-3 plays a crucial role in the outward currents elicited by eucalyptol and methyl salicylate-elicited inward currents suggest that inhibitors and agonists bind to the same primary binding site. As previously demonstrated in studies with an OR from *Drosophila melanogaster* [28] and pheromone receptors from *Ostrinia* species [29], TM3 is part of receptor binding pockets, with residue 148 in *Ostrinia* being a specificity determinant [29]. Recently, these findings have been corroborated by the report of the first structure of an insect odorant receptor, MhraOR5 [30], showing that multiple residues from TM-3 (referred to as S-3) interact with ligands, including one forming a lid for the binding pocket. More importantly, it has been demonstrated that mutation of Ser-151 in TM-3 to Ala caused an increase in baseline activity, thus indicating that Ser-151 and other residues stabilize the close conformation of the receptor [30]. Recently, we reported that another mosquito odorant receptor, CquiOR27, displays dual current directions [22]. Interestingly, some dimethylphenol isomers elicited inward currents, while others generated outward currents. We then surmised that the recorded currents in the reverse direction (outward currents) could be derived from the binding of inhibitors to the orthosteric binding site. In this scenario, binding to inhibitors would close the constitutively open receptor's ion channels [30–32], i.e., binding to an inhibitor might shift the equilibrium of the open <=> close conformations towards the inactive (closed) conformation of the receptor, thus reducing the spontaneous activity. In summary, these new findings suggest that inhibitory compounds might be inverse agonists that bind to the primary binding site and switch off receptors, thus reducing the spontaneous activity and shifting the "baseline" in TEVC recordings.

Co-applications of an agonist and an inverse agonist.

Previously, we had demonstrated that when co-applied with an agonist, a mosquito odorant receptor inhibitor reduced the agonist-elicited inward currents in a dose-dependent fashion, i.e., as the concentrations of the inhibitor increased, the responses of the co-applied agonist decreased. [15,22]. We asked whether/how continuous exposure to an inhibitory compound would affect a receptor response to an agonist. The responses of CquiOR32/CquiOrco-expressing oocytes to 0.1 mM methyl salicylate were recorded five times. Then, the same oocytes were exposed to a perfusion buffer containing 0.1 μM eucalyptol. Once the baseline, which shifted upwards, stabilized, we recorded the responses to 0.1 mM methyl salicylate while the receptors were continuously exposed to eucalyptol (0.1 μM). Similarly, the protocol was repeated with recordings using a control perfusion buffer and then a higher concentration of eucalyptol (1, 10, or 100 μM) while keeping the dose of methyl salicylate constant, 100 μM = 0.1 mM. Data were normalized to allow comparisons using multiple oocytes and different batches of the perfusion buffers with or without eucalyptol at various concentrations. There were no significant differences (N=17-21, P>0.05, Wilcoxon matched-pairs signed-rank test) between the methyl salicylate responses recorded from CquiOR32/CquiOrco-expressing oocytes in the absence of eucalyptol as compared to 0.1, 1, or 10 μM eucalyptol (Fig. 3A). However, the methyl salicylate responses reduced significantly when the receptors were continuously exposed to 100 μM of eucalyptol, i.e., the same agonist dose (N=18, P=0.0019, Wilcoxon matched-pairs signed-rank test) (Fig. 3A). Similar results were obtained using CquiOR32V2/CquiOrco-expressing oocytes (Fig. 3B). Methyl salicylate currents recorded in the absence of eucalyptol were not significantly different from those obtained with the receptors exposed to eucalyptol at 0.1, 1, or 10 μM (N=10-12,

P>0.05, Wilcoxon matched-pairs signed-rank test). There was a significant difference when comparing methyl salicylate-elicited responses in the absence of eucalyptol with those recorded with the receptors exposed to eucalyptol at 100 μM (N=8, P>0.0078, Wilcoxon matched-pairs signed-rank test) (Fig. 3B). Although the reduction in responses observed with CquiOR32V2 (Fig. 3B) was larger than with CquiOR32 (Fig. 3A) when eucalyptol and methyl salicylate were co-applied at the same dose, there was no significant difference between the reduced responses observed with the two variants of the receptor (46.3±9.8 and 31.0±7.6% for CquiOR32V2 and CquiOR32, respectively, N=8-18, P=0.2563, unpaired t-test).

It is conceivable that methyl salicylate and eugenol bind to different binding pockets, with eucalyptol having a lower affinity. However, this dataset combined with the variants studies (see above) support the hypothesis that eucalyptol and methyl salicylate compete for the same binding pocket.

Current-voltage relationships suggest that eucalyptol binding reduces cation influx.

We generated I-V curves for CquiOR32V with currents induced by methyl salicylate or eucalyptol while clamping the voltage at −80, −60, −40, −20, 0, 20, and 40 mV. Then, we compared these curves with I-V relationships obtained with sodium chloride in the perfusion buffer replaced by N-methyl-D-glucamine chloride (NMG, sodium-free buffer) (Fig. 4) or sodium gluconate (chloride-free buffer) (Figs. 3). These reagents serve to infer channel permeability to cations and anions, respectively, given that the former is a bulky impermeable mono cation, and the latter is a bulky, non-permeable source of anions. The voltage dependence of methyl salicylate-induced currents shifted to the left when the perfusion buffer was replaced with an NMG buffer (Fig. 4A). This observation is not surprising given that insect odorant receptors are known to be non-selective cation channels [33–36]. A linearization of these I-V curves showed that the reverse potential (V_{rev}) shifted from −28.1±3.1 mV to −59.8±7.7 mV, a shift consistent with cation channels. The curves obtained with the voltage-dependent eucalyptol-elicited currents using the standard perfusion buffer and the sodium-free NMG buffer showed a left shift, thus strongly suggesting that these currents involve cation channels (Fig 4B). The reversal potential calculated by linearization changed from −21.4±2.6 mV (sodium buffer) to −49.8±3.8 mV (sodium-free buffer). At −80 mV (the standard holding voltage for oocyte recordings), eucalyptol in the regular perfusion buffer induced robust outward currents: 224.4±25 nA (N=11), whereas as in NMG the currents were almost entirely abolished: 27.6±3.6 nA (N=12, P<0.0001, two-tailed, unpaired t-test) (Fig. 4B). Of note, insect ORs are non-selective cation channels [33–36], and the NMG buffer contains K^+, Ca^{++}, and Mg^{++} at 2, 1.8, and 5 mM, respectively. These data show that the eucalyptol-induced currents decreased significantly in an environment with a low extracellular concentration of permeable cations. In short, these findings suggest that the observed upward deflections (outward currents) are mediated at least in part by cation channels. A plausible explanation is that upon eucalyptol binding to CquiOR32V2, the receptor equilibrium shifts towards the closed conformation, thus reducing spontaneous activities (influx of cations).

The I-V curves obtained with gluconate buffer shifted to the right with methyl salicylate-elicited currents (Figs. 3A, −28.1±3.1 mV to −11.7±3.3 mV) and eucalyptol-elicited currents (Figs. 3B, −21.4±2.6 mV to −3.8±1.7 mV; V_{rev} values calculated with a linear approximation). Because these data suggest permeability to chloride, we investigated whether the *Xenopus* Ca^{++}-activated chloride channel [37] xTMEM16A [38] play a role in the outward currents elicited by eucalyptol. First, we tested CquiOR32V-expressing oocytes (receptor alone), and they did not elicit currents when challenged with OLC12, eucalyptol, or methyl salicylate at 0.01, 0.1., or 1 mM. Likewise, CquiOrco-expressing oocytes (coreceptor alone) did not respond to eucalyptol or methyl salicylate. As expected [25,36,39], CquiOrco-expressing oocytes generated inward currents when challenged with OLC12. Lastly, we recorded currents from CquiOR32V2/CquiOrco-expressing oocytes with perfusion buffers devoid of Ca^{++}. The relatively larger eucalyptol-elicited outward currents than methyl salicylate-generated inward currents were observed in regular (Ca^{++}-containing perfusion buffer), with Ba^{++} replacing Ca^{++}, and in Ca^{++}-free buffers (Figs. 4). It is, therefore, unlikely that xTNMP16A is involved. It is conceivable that CquiOR32V2/CquiOrco ion channels may be permeable to chloride, but it would not explain the eucalyptol-elicited upward deflection (outward currents). The measured outward currents elicited by eucalyptol at −80 mV were significantly higher when the perfusion buffer was devoid of chloride (347±44 nA) than in a standard (chloride) buffer (224±25 nA, N=11, P=0.0288, two-tailed, unpaired t-test). Under gluconate buffer, chloride currents would be elicited by Cl^- efflux (inward currents) given the higher intracellular Cl^- concentration (54 mM) in *Xenopus* oocytes [40]. We, therefore, concluded that the outward currents are mediated mainly by a reduction of sodium influx.

4. Overall conclusions

Three lines of experimental evidence support three conclusions: (1) methyl salicylate and eucalyptol may act on the same orthosteric binding pocket; (2) they affect the same cation channels; and (3) binding of the agonist leads to an increase in sodium influx, whereas antagonist binding reduces the spontaneous activity. We showed that substitutions in two residues in the predicted binding pocket of a mosquito odorant receptor, CquiOR32, affect the responses of both an agonist and an inhibitory compound thus suggesting they act on the same binding site. Experiments with the receptor exposed to the inhibitory compound showed that higher doses of the inhibitor are necessary to cause a significant reduction in the agonist response, consistent with a possible mechanism of competitive binding. Analysis of current-voltage relationships showed that current elicited by both agonist and inhibitory compounds are affected by extracellular sodium concentrations, therefore, suggesting that the same cation channels are involved. We then concluded that eucalyptol is an inverse agonist. As previously reported, mosquitoes' repellency response to methyl salicylate is negatively affected by eucalyptol [15]. This eucalyptol-mediated behavioral antagonism is likely mediated by a competitive binding mechanism. We hypothesize that eucalyptol and methyl salicylate act on the same binding site, with the former causing a reduction in the receptor's spontaneous activity and the latter increasing neuronal activity.

Supplementary Material

Refer to Web version on PubMed Central for supplementary material.

Acknowledgments

Abbreviations

ORN	Olfactory receptor neuron
OR	odorant receptor
TEVC	two-electrode voltage-clamp
OLC12	Orco ligand candidate
NMG	N-methyl-D-glucamine chloride
CquiOR32V2	variant 2 of the odorant receptor 32
I-V	current-voltage

References

[1]. Leal WS, 3.11 - Mechanism of Action of Insect Pheromones and Other Semiochemicals, in: Liu H-W, Begley TP (Eds.) Comprehensive Natural Products III, Elsevier, Oxford, 2020, pp. 222–236.

[2]. Chang H, Liu Y, Ai D, Jiang X, Dong S, Wang G, A Pheromone Antagonist Regulates Optimal Mating Time in the Moth Helicoverpa armigera, Current Biology 27 (2017) 1610–1615.e1613. 10.1016/j.cub.2017.04.035. [PubMed: 28528905]

[3]. Baker TC, Cossé AA, Todd JL, Behavioral antagonism in the moth Helicoverpa zea in response to pheromone blends of three sympatric heliothine moth species is explained by one type of antennal neuron, Ann N Y Acad Sci 855 (1998) 511–513. 10.1111/j.1749-6632.1998.tb10616.x. [PubMed: 10049230]

[4]. Zhu J, Park KC, Baker TC, Identification of odors from overripe mango that attract vinegar flies, Drosophila melanogaster, J Chem Ecol 29 (2003) 899–909. 10.1023/a:1022931816351. [PubMed: 12775150]

[5]. Stensmyr MC, Dweck HK, Farhan A, Ibba I, Strutz A, Mukunda L, Linz J, Grabe V, Steck K, Lavista-Llanos S, Wicher D, Sachse S, Knaden M, Becher PG, Seki Y, Hansson BS, A conserved dedicated olfactory circuit for detecting harmful microbes in Drosophila, Cell 151 (2012) 1345–1357. 10.1016/j.cell.2012.09.046. [PubMed: 23217715]

[6]. Syed Z, Leal WS, Acute olfactory response of Culex mosquitoes to a human- and bird-derived attractant, Proc Natl Acad Sci U S A 106 (2009) 18803–18808. 10.1073/pnas.0906932106. [PubMed: 19858490]

[7]. Leal WS, Barbosa RM, Xu W, Ishida Y, Syed Z, Latte N, Chen AM, Morgan TI, Cornel AJ, Furtado A, Reverse and conventional chemical ecology approaches for the

development of oviposition attractants for *Culex mosquitoes*, PLoS One 3 (2008) e3045. 10.1371/journal.pone.0003045. [PubMed: 18725946]

[8]. Paluch G, Bartholomay L, Coats J, Mosquito repellents: a review of chemical structure diversity and olfaction, Pest Manag Sci 66 (2010) 925–935. 10.1002/ps.1974. [PubMed: 20623705]

[9]. Haupt SS, Sakurai T, Namiki S, Kazawa T, Kanzaki R, Olfactory Information Processing in Moths, in: Menini A (Ed.) The Neurobiology of Olfaction, Boca Raton (FL), 2010.

[10]. Galizia CG, Sachse S, Odor Coding in Insects, in: Menini A (Ed.) The Neurobiology of Olfaction, Boca Raton (FL), 2010.

[11]. Hildebrand JG, Olfactory control of behavior in moths: central processing of odor information and the functional significance of olfactory glomeruli, J Comp Physiol A 178 (1996) 5–19. 10.1007/BF00189586. [PubMed: 8568724]

[12]. Kaissling KE, Pheromone Reception in Insects: The Example of Silk Moths, in: Mucignat-Caretta C (Ed.) Neurobiology of Chemical Communication, Boca Raton (FL), 2014.

[13]. Nikonov AA, Leal WS, Peripheral coding of sex pheromone and a behavioral antagonist in the Japanese beetle, *Popillia japonica*, J Chem Ecol 28 (2002) 1075–1089. [PubMed: 12049228]

[14]. Su CY, Menuz K, Reisert J, Carlson JR, Non-synaptic inhibition between grouped neurons in an olfactory circuit, Nature 492 (2012) 66–71. 10.1038/nature11712. [PubMed: 23172146]

[15]. Xu P, Choo YM, Chen Z, Zeng F, Tan K, Chen TY, Cornel AJ, Liu N, Leal WS, Odorant inhibition in mosquito olfaction, iScience 19 (2019) 25–38. 10.1016/j.isci.2019.07.008. [PubMed: 31349189]

[16]. Ye Z, Liu F, Liu N, Olfactory Responses of Southern House Mosquito, Culex quinquefasciatus, to Human Odorants, Chem Senses 41 (2016) 441–447. 10.1093/chemse/bjv089. [PubMed: 26969630]

[17]. Tauxe GM, MacWilliam D, Boyle SM, Guda T, Ray A, Targeting a dual detector of skin and CO_2 to modify mosquito host seeking, Cell 155 (2013) 1365–1379. 10.1016/j.cell.2013.11.013. [PubMed: 24315103]

[18]. Ghaninia M, Ignell R, Hansson BS, Functional classification and central nervous projections of olfactory receptor neurons housed in antennal trichoid sensilla of female yellow fever mosquitoes, Aedes aegypti, Eur J Neurosci 26 (2007) 1611–1623. 10.1111/j.1460-9568.2007.05786.x. [PubMed: 17880395]

[19]. Wu S-T, Chen J-Y, Martin V, Ng R, Zhang Y, Grover D, Greenspan RJ, Aljadeff J, Su C-Y, Valence opponency in peripheral olfactory processing, Proceedings of the National Academy of Sciences 119 (2022) e2120134119. 10.1073/pnas.2120134119.

[20]. Xu P, Zeng F, Bedoukian RH, Leal WS, DEET and other repellents are inhibitors of mosquito odorant receptors for oviposition attractants, Insect Biochem Mol Biol 113 (2019) 103224. 10.1016/j.ibmb.2019.103224. [PubMed: 31446031]

[21]. Lee Y, Seifert SN, Nieman CC, McAbee RD, Goodell P, Fryxell RT, Lanzaro GC, Cornel AJ, High degree of single nucleotide polymorphisms in California Culex pipiens (Diptera: Culicidae) sensu lato, J Med Entomol 49 (2012) 299–306. 10.1603/me11108. [PubMed: 22493847]

[22]. Xu P, Choo Y-M, An S, Leal GM, Leal WS, Mosquito odorant receptor sensitive to natural spatial repellents and inhibitory compounds, bioRxiv (2022) 2022.2001.2019.476929. 10.1101/2022.01.19.476929.

[23]. Xu P, Wen X, Leal WS, CO_2 per se activates carbon dioxide receptors, Insect Biochem Mol Biol 117 (2020) 103284. 10.1016/j.ibmb.2019.103284. [PubMed: 31760135]

[24]. Choo YM, Xu P, Hwang JK, Zeng F, Tan K, Bhagavathy G, Chauhan K, Leal WS, Reverse chemical ecology approach for the identification of an oviposition attractant for Culex quinquefasciatus, Proc Natl Acad Sci U S A in press (2018).

[25]. Chen S, Luetje CW, Identification of new agonists and antagonists of the insect odorant receptor co-receptor subunit, PLoS One 7 (2012) e36784. 10.1371/journal.pone.0036784. [PubMed: 22590607]

[26]. Taylor RW, Romaine IM, Liu C, Murthi P, Jones PL, Waterson AG, Sulikowski GA, Zwiebel LJ, Structure-activity relationship of a broad-spectrum insect odorant receptor agonist, ACS Chem Biol 7 (2012) 1647–1652. 10.1021/cb300331z. [PubMed: 22924767]

[27]. Reynolds SM, Kall L, Riffle ME, Bilmes JA, Noble WS, Transmembrane topology and signal peptide prediction using dynamic bayesian networks, PLoS Comput Biol 4 (2008) e1000213. 10.1371/journal.pcbi.1000213. [PubMed: 18989393]

[28]. Nichols AS, Luetje CW, Transmembrane segment 3 of Drosophila melanogaster odorant receptor subunit 85b contributes to ligand-receptor interactions, J Biol Chem 285 (2010) 11854–11862. 10.1074/jbc.M109.058321. [PubMed: 20147286]

[29]. Leary GP, Allen JE, Bunger PL, Luginbill JB, Linn CE Jr., Macallister IE, Kavanaugh MP, Wanner KW, Single mutation to a sex pheromone receptor provides adaptive specificity between closely related moth species, Proc Natl Acad Sci U S A 109 (2012) 14081–14086. 10.1073/pnas.1204661109. [PubMed: 22891317]

[30]. Del Marmol J, Yedlin MA, Ruta V, The structural basis of odorant recognition in insect olfactory receptors, Nature 597 (2021) 126–131. 10.1038/s41586-021-03794-8. [PubMed: 34349260]

[31]. Cao LH, Yang D, Wu W, Zeng X, Jing BY, Li MT, Qin S, Tang C, Tu Y, Luo DG, Odor-evoked inhibition of olfactory sensory neurons drives olfactory perception in Drosophila, Nat Commun 8 (2017) 1357. 10.1038/s41467-017-01185-0. [PubMed: 29116083]

[32]. Pask GM, Bobkov YV, Corey EA, Ache BW, Zwiebel LJ, Blockade of insect odorant receptor currents by amiloride derivatives, Chem Senses 38 (2013) 221–229. 10.1093/chemse/bjs100. [PubMed: 23292750]

[33]. Sato K, Pellegrino M, Nakagawa T, Nakagawa T, Vosshall LB, Touhara K, Insect olfactory receptors are heteromeric ligand-gated ion channels, Nature 452 (2008) 1002–1006. 10.1038/nature06850. [PubMed: 18408712]

[34]. Smart R, Kiely A, Beale M, Vargas E, Carraher C, Kralicek AV, Christie DL, Chen C, Newcomb RD, Warr CG, Drosophila odorant receptors are novel seven transmembrane domain proteins that can signal independently of heterotrimeric G proteins, Insect Biochem Molec 38 (2008) 770–780. 10.1016/j.ibmb.2008.05.002.

[35]. Wicher D, Schafer R, Bauernfeind R, Stensmyr MC, Heller R, Heinemann SH, Hansson BS, Drosophila odorant receptors are both ligand-gated and cyclic-nucleotide-activated cation channels, Nature 452 (2008) 1007–1011. 10.1038/nature06861. [PubMed: 18408711]

[36]. Pask GM, Jones PL, Rutzler M, Rinker DC, Zwiebel LJ, Heteromeric Anopheline odorant receptors exhibit distinct channel properties, PLoS One 6 (2011) e28774. 10.1371/journal.pone.0028774. [PubMed: 22174894]

[37]. Hartzell C, Putzier I, Arreola J, Calcium-activated chloride channels, Annu Rev Physiol 67 (2005) 719–758. 10.1146/annurev.physiol.67.032003.154341. [PubMed: 15709976]

[38]. Schroeder BC, Cheng T, Jan YN, Jan LY, Expression cloning of TMEM16A as a calcium-activated chloride channel subunit, Cell 134 (2008) 1019–1029. 10.1016/j.cell.2008.09.003. [PubMed: 18805094]

[39]. Jones PL, Pask GM, Rinker DC, Zwiebel LJ, Functional agonism of insect odorant receptor ion channels, Proc Natl Acad Sci U S A 108 (2011) 8821–8825. 10.1073/pnas.1102425108. [PubMed: 21555561]

[40]. Lotan I, Dascal N, Cohen S, Lass Y, Adenosine-induced slow ionic currents in the Xenopus oocyte, Nature 298 (1982) 572–574. 10.1038/298572a0. [PubMed: 6285198]
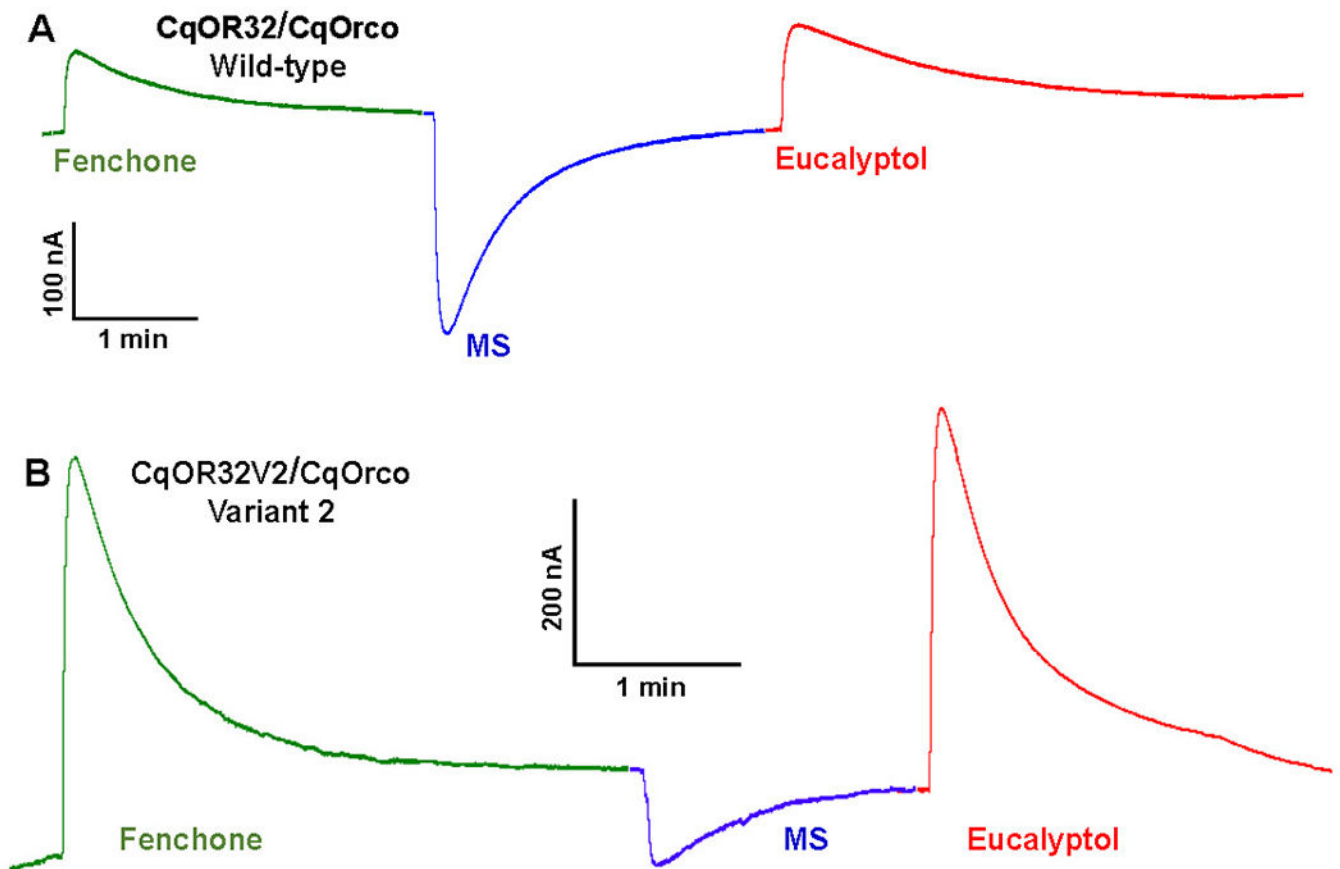
Fig. 1. Recordings obtained with oocytes co-expressing CquiOR32 or CquiOR32V2 with CquiOrco.

(A) Methyl salicylate-elicited inward currents recorded with CquiOR32/CquiOrco-expressing oocytes were relatively more prominent than the outward currents elicited by fenchone and eucalyptol. By contrast, (B) CquiOR32V2/CquiOrco-expressing oocytes generated comparatively larger inhibitory currents (elicited by fenchone and eucalyptol) than methyl salicylate-elicited inward currents. Dose: 1 mM.
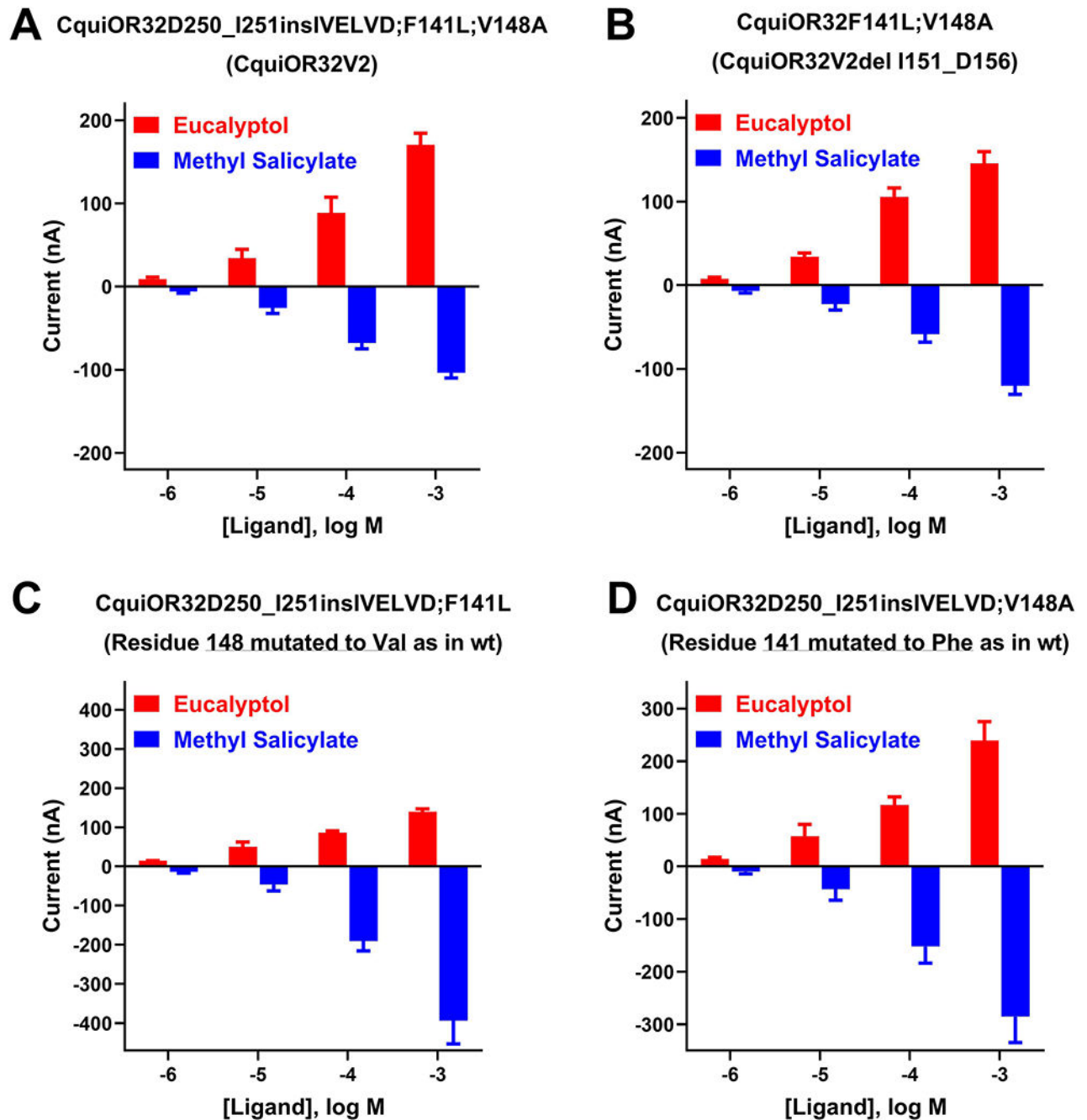
Fig. 2. Quantification of inward and outward currents recorded with CquiOR32V2 and two mutants.

For clarity, the bars are displayed in the same direction of the currents they elicited: methyl salicylate (blue, inward currents, downward) and eucalyptol (red, outward currents) (Fig. 1). Currents recorded with (A) CquiOR32V2/CquiOrco-expressing oocytes (V2 response) and (B) CquiOR32F141L;V148A (V2 without the insert). (C) Responses recorded with V2 mutated to rescue residue 148. Thus, Ala-148 in A was mutated to Val (as in the wild-type version of the receptor). (D) Responses recorded with V2 mutated to rescue residue 141. This mutation differs from A in that Leu-141 was mutated into Phe.
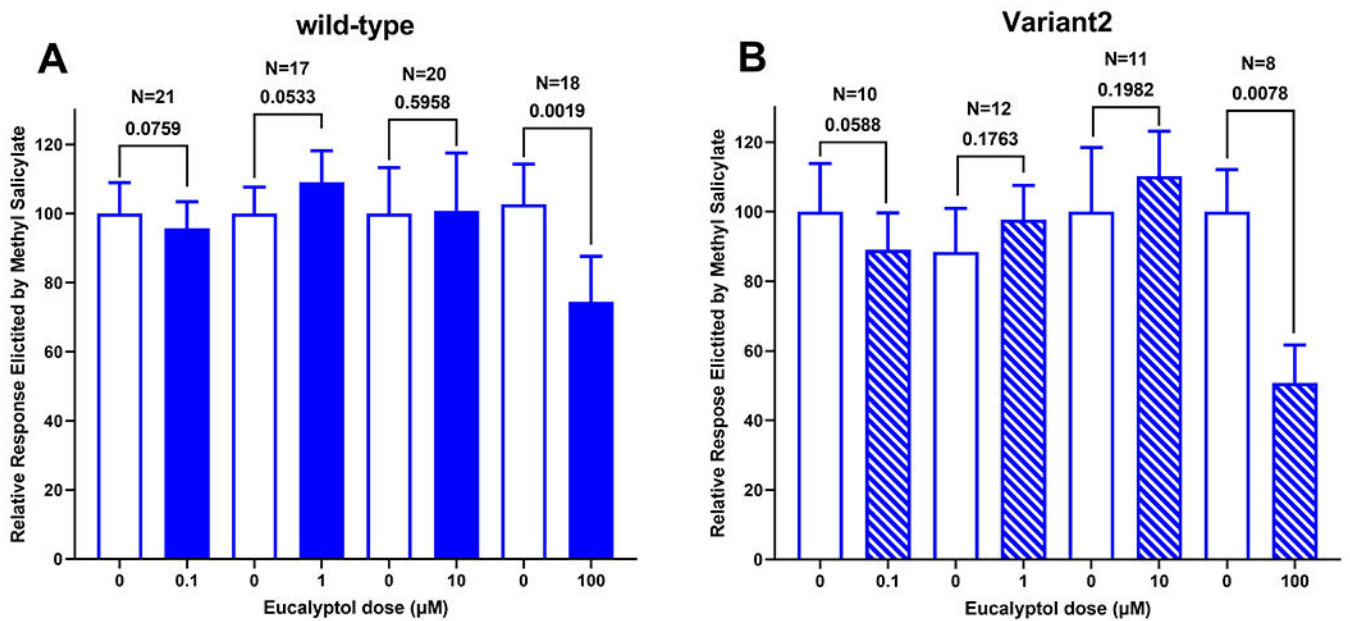
Fig. 3. Quantification of the responses elicited by methyl salicylate presented either alone (empty bars) or during continuous exposure to eucalyptol (filled bars).

Methyl salicylate responses were recorded with (A) CquiOR32/CquiOrco- and (B) CquiOR32V2/CquiOrco-expressing oocytes, i.e., wild-type and Variant2, respectively. For each eucalyptol dose tested (0.1, 1, 10, and 100 μM), a control was obtained before the standard perfusion buffer was replaced with a perfusion buffer containing eucalyptol. The methyl salicylate responses were normalized separately, using the mean response to each control.
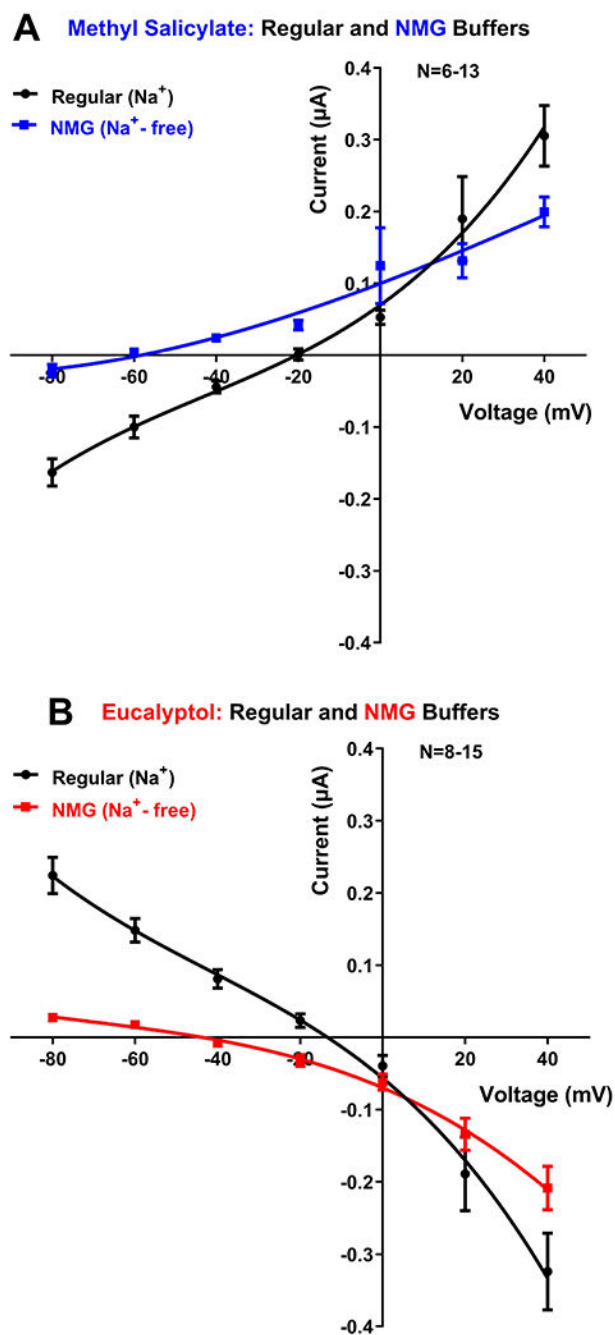
Fig. 4. Current-voltage relationships obtained with CquiOR32V2/CquiOrco-expressing oocytes.
(A) Voltage-dependent methyl salicylate-elicited currents using a standard perfusion buffer (black trace) and in a Na$^+$-free buffer (blue trace). (B) Voltage-dependent eucalyptol-elicited currents using a standard perfusion buffer (black trace) and in a Na$^+$-free buffer (red trace) For clarity, the two graphics were displayed on the same Y scale (−0.4 to 0.4 µA). A linear approximation calculated reverse potentials, but the displayed curves were fit using a centered third order polynomial.